IEEE Access
Multidisciplinary | Rapid Review | Open Access Journal

Received February 11, 2022, accepted March 18, 2022, date of publication March 31, 2022, date of current version April 11, 2022.

Digital Object Identifier 10.1109/ACCESS.2022.3163845

GlauCUTU: Time Until Perceived Virtual Reality Perimetry With Humphrey Field Analyzer Prediction-Based Artificial Intelligence

PATTHAPOL KUNUMPOL[1,2], (Member, IEEE), NICHAPA LERTHIRUNVIBUL[1,3], PHONGPHAN PHIENPHANICH[1,2], (Member, IEEE), ADIREK MUNTHULI[1,2], (Student Member, IEEE), KANJAPAT TEMAHIVONG[1,4,5], VISANEE TANTISEVI[4,5], ANITA MANASSAKORN[4,5], SUNEE CHANSANGPETCH[4,5], RATH ITTHIPANICHPONG[4,5], KITIYA RATANAWONGPHAIBUL[4,5], PRIN ROJANAPONGPUN[4,5], AND CHARTURONG TANTIBUNDHIT[1,2], (Member, IEEE)

[1]Center of Excellence in Intelligent Informatics, Speech and Language Technology, and Service Innovation (CILS), Thammasat University, Rangsit Campus, Khlong Luang, Bangkok, Pathum Thani 12120, Thailand
[2]Department of Electrical and Computer Engineering, Faculty of Engineering, Thammasat University, Rangsit Campus, Khlong Luang, Bangkok, Pathum Thani 12120, Thailand
[3]Faculty of Medicine, Thammasat University, Rangsit Campus, Khlong Luang, Bangkok, Pathum Thani 12120, Thailand
[4]Glaucoma Research Unit, Department of Ophthalmology, Faculty of Medicine, Chulalongkorn University, Bangkok 10330, Thailand
[5]King Chulalongkorn Memorial Hospital, Thai Red Cross Society, Pathumwan, Bangkok 10330, Thailand

Corresponding author: Charturong Tantibundhit (tchartur@engr.tu.ac.th)

The work of Patthapol Kunumpol was supported by the Scholarship from the Faculty of Engineering, Thammasat University. This work was supported by the Program Management Unit for Competitiveness, Office of National Higher Education, Science, Research and Innovation Policy Council together with work Udon Thani Cancer Hospital Foundation.

This work involved human subjects or animals in its research. Approval of all ethical and experimental procedures and protocols was granted by the Chulalongkorn Institutional Review Board under Application No. 715/61.

ABSTRACT The increasing prevalence of glaucomatous optic neuropathy, which can result in permanent blindness (visual impairment), accentuates the importance of screening and early diagnosis for prevention of blindness. GlauCUTU, a novel time until perceived (TUP) visual field (VF) testing, utilizes a portable virtual reality (VR) headset with visual stimulus that progressively increases in intensity to detect VF defects. GlauCUTU was evaluated on participants with normal visual fields and those with early, moderate, and severe glaucoma. Responses were collected in terms of time until response (TUR). TUR was used to calculate TUP and reported in terms of GlauCUTU sensitivity. False positives were detected with pretest and latency analysis using reaction time (RT). In addition, a novel automated transformation was developed to convert GlauCUTU sensitivity into HFA sensitivity using machine learning (ML) and deep learning (DL) algorithms. Visual field index (VFI) was generated from HFA sensitivity to determine severity of glaucoma. The VFI results were evaluated using post-hoc analysis from two-way analysis of variance (ANOVA). Results demonstrate no significant difference ($p=0.073$) between Humphrey visual field analyzer (HFA) and GlauCUTU with machine learning transformation (GlauCUTU-ML) in all glaucoma stages. However, there was a significant difference between HFA and GlauCUTU with deep learning transformation (GlauCUTU-DL) in severe glaucoma ($p<0.050$). GlauCUTU-ML generates the lowest root mean square error (RMSE) of 4.92. Meanwhile, GlauCUTU-DL yields the highest Pearson's r correlation coefficient with HFA of 0.74, but produces the highest RMSE of 6.31. Comparison between three expert ophthalmologists' grading of glaucomatous eyes on GlauCUTU-ML and HFA aligns with the majority voting with an average agreement of 0.83, which is highly reliable. All in all, the portable and inexpensive GlauCUTU perimetry system introduces the use of TUP for VF evaluation with results comparable to HFA. GlauCUTU proves to be a promising method to increase accessibility to glaucoma screening, particularly in low-resource setting countries.

INDEX TERMS Virtual reality, glaucoma, visual defect, visual field test, portable perimetry.

The associate editor coordinating the review of this manuscript and approving it for publication was Seifedine Kadry.

I. INTRODUCTION

Glaucoma optic neuropathy is a leading cause of permanent vision loss that affects about 60 million people worldwide and is expected to inflict 111.8 million people by 2040 [1]. The disease damages retinal ganglion cells and retinal nerve fibers at the optic nerve head (ONH) causing irreversible blindness. Fortunately, screening for early diagnosis of glaucoma can help prevent blindness [1]–[3]. However, accessibility and quality of glaucoma screening, especially in rural areas, are limited by several factors. For one, there is an average of 1.52 ophthalmologist per 100,000 persons in Thailand; however, there are no ophthalmologists or ophthalmic tools in many rural areas [4]. Consequently, glaucoma diagnosis and treatment are delayed. Therefore, enhanced ophthalmic tools may increase accessibility to screening and prevent irreversible blindness from glaucoma.

Clinical manifestations of glaucoma include glaucomatous optic neuropathy and visual field defects [5]. Screening comprises of ONH examination through fundus imaging or optical coherence tomography (OCT) and visual field (VF) evaluation [5]. Glaucomatous VF changes include nasal step defect, temporal wedge VF loss, arcuate defect, tunnel vision, and severe VF defect sparing a crestcent-shape pattern in the temporal area [6]. VF can be evaluated using standard automated perimetry (SAP) such as HFA.

Humphrey visual field analyzer (HFA), the current clinical standard for assessing VF defects, is crucial for diagnosis and monitoring of multiple ophthalmic and neurologic diseases including glaucoma [7], [8]. In the HFA (Zeiss Humphrey Systems, Dublin, Calif) test [9], [10], subjects react to the stimulus presented on a 2D plane up to $\pm 30^{\circ}$ temporally and nasally by clicking on a button. Visual field defects are detected with contrast sensitivity [11]. Contrast sensitivity determines the light level which can be detected by the patient with a 50% probability.

Although the HFA device is widely used, it is large, immobile, and expensive, which limits its use in rural areas [12]. The HFA requires patients to maintain a fixed head position, which can be challenging for the elderly and bedridden patient [13]. Also, SAP entails higher subject concentration as several minutes of fixation on the target is required. Hence, the subject's alertness and reaction to the visual stimuli can lead to variability and fluctuation within the same assessment or between examinations [7].

As HFA has high costs and is immobile, there are only a few HFA devices in Thailand, which are mostly located in big cities. Lack of access to HFA limits accessibility to early glaucoma diagnosis. Therefore, the use of a glaucoma screening device can help filter for cases that necessitate diagnosis with HFA leading to faster and earlier diagnosis. A possible screen tool are VR glasses, which are portable and inexpensive.

Furthermore, VR headsets allow subjects to freely move their heads making the device more suitable for the elderly and bedridden patients and for at-home glaucoma monitoring [13], [14]. VR perimetry was reported as more comfortable than the standard HFA [7], [13], [14]. Moreover, the portable VR headset is especially beneficial during the coronavirus disease 2019 (COVID-19) outbreak as it enables home-isolated glaucoma detection and monitoring without having to visit the hospital [14], [15].

In recent years, there are multiple studies on the use of VR perimetry devices for detection of VF defects such as glaucoma. Tsapakis *et al.* created an automated perimetry test using a commercially available VR device, Trust EXOS 3D VR glasses, and a smartphone. Comparison between their proposed method and the HFA in glaucoma patients indicated high correlation coefficient [13]. Another modality created by Saccà *et al.* is a compact, head-mounted, and eye-tracking VR perimeter known as VirtualEye [7]. Although the VirtualEye evaluates retinal sensitivity, there was a systemic shift in sensitivities between VirtualEye and HFA.

Mees *et al.* introduced a head-mounted VR perimetry device known as the C3 fields analyzer, which was moderately effective at recognizing glaucoma patients, but the VF results did not match those of HFA [8]. Most recently, Sipatchin *et al.* investigated the feasibility of commercially available VR headset equipped with eye-tracking features for bedside VF assessments [16]. Recent VR perimetry modalities have been developed that can potentially become portable alternatives to the conventional VF tests [14], [17]–[19]. Razeghinejad *et al.* created a head-mounted perimetry known as the VisuALL, which demonstrated high diagnostic performance by producing results with significant correlation to those of the HFA in both normal and glaucoma patients, but it had a longer test duration than the HFA [18]. Despite the growing interest and potential clinical use of VR in perimetry, the modality is still in its investigational phase and has several limitations.

To the best of our knowledge, previous VR perimetry tests can differentiate between glaucoma patients and normal subjects, but results differ from those of HFA. In our previous work, we developed a VR perimetry test that assesses participant's RT which is reportedly higher in glaucoma patients than in normal subjects [20]. In this study, we use the term time until response (TUR) instead of RT, which was used in our previous work, as TUR better demonstrates the variable. In perimetry tests, RT is generally defined as the time between the onset of the stimulus and the patient's response using suprathreshold perimetry [21]. However, in GlauCUTU, the stimulus is initially presented at its lowest intensity. Then, the intensity gradually increases until the participant perceives and presses on the clicker. Hence, TUR is the duration from presentation of stimulus with the lowest intensity until the participant responds by pressing on the clicker.

GlauCUTU can be used for glaucoma screening by measuring TUP and reporting in GlauCUTU sensitivity. However, our perimetry results cannot be compared with HFA, which makes it difficult for clinicians to use GlauCUTU's data to assess visual field defects [20]. Currently, there are no

available system capable of predicting HFA sensitivity from TUR. In this work, we developed machine learning (ML) and deep learning (DL)-based transformation algorithms that allow conversion from GlauCUTU sensitivity to HFA sensitivity in decibel (dB) units. As accessibility to HFA in low-resource countries is limited, a novel VR technology that is portable and inexpensive has the potential to improve glaucoma care in countries such as Thailand. Our goal is to enhance the GlauCUTU VR system's reliability and applicability for glaucoma screening and glaucoma severity classification with results clinically interpretable as those of HFA.

The main contributions of this paper are as follows:

1) A novel automated transformation using ML and DL algorithms are developed to estimate HFA sensitivity from GlauCUTU sensitivity and map corresponding visual field with high correlation using the GlauCUTU perimetry system.
2) GlauCUTU, a VR perimetry system, enables glaucoma screening with high reliability agreement with clinician's interpretation of HFA results, and has a shorter test duration by approximately 310 seconds than the HFA.
3) Inclusion of pretest and latency tests as reliability index through detection of false positive results, which can help enhance accuracy of results.
4) A customized VR perimetry system that is portable and inexpensive. The method can be operated in any lighting environment, unlike the conventional HFA that requires a dark setting. GlauCUTU is proposed as an alternative glaucoma screening tool in low-resource settings and for elderly and debilitated patients.

The organization of this paper is structured as follows: Section II describes the GlauCUTU's design and implementation. Section III demonstrates the automated conversion of GlauCUTU sensitivity into HFA sensitivity values. Section IV shows the experimental design and setup. Sections V and VI show the results, discussion, and future works, respectively. Section VII is acknowledgement.

II. GlauCUTU DESIGN & IMPLEMENTATION

This section aims to provide details regarding the hardware and software features of GlauCUTU. The modular design of GlauCUTU accommodates user's convenience and ease of access with cutting-edge technologies.

A. HARDWARE FEATURES

The novel technology of 3D printing enables rapid and reliable production of GlauCUTU that can be personalized for each patient's unique physiology [22]. Rather than using commercially-available VR glasses, we created our own VR device to enable adjustable pupillary distance and reduce costs. The silicone rubber incorporated in GlauCUTU's VR glasses has received silicone food grade [23], while other materials used to create the headset were proven safe for use [24]. Our perimetry VR headset utilized two separate liquid crystal display (LCD) systems to provide the user with

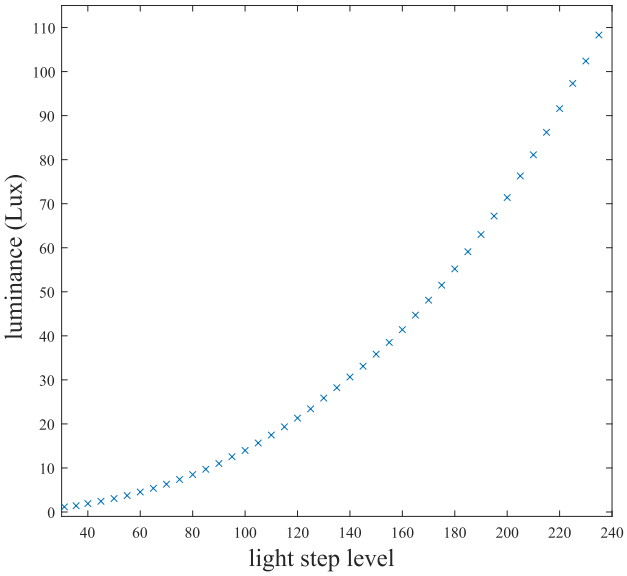

FIGURE 1. The relationship between empirical screen luminance in lux (y-axis) and light step level (x-axis).

a binocular view, which enables adequate positioning and increases the subject's field of view. A wide field of view reduces lens rim artifact (LRA), which can mimic nasal step scotoma seen in glaucoma [13]. The system reduced distortion from ambient light as each module includes a convex lens and a monitor display that can be adjusted to accommodate each individual eye with variations in pupillary distance [25].

The reasons for choosing LCD over Organic Light Emitting Diode (OLED) for the display screen were the lower costs and the benefits of backlighting, which increased visual comfort and reduced test-induced eye fatigue [26]. The contrast ratio, a ratio between the brightest white and the darkest black produced by the Sharp LCD module no. LS029B3SX02, was quantified with Extech EA31 EasyView Light Meter [13]. The EA31 EasyView Light Meter has a maximum resolution of 0.01 Fc/Lux [27] with a calibration certificate CAL03035-20 from Industrial Calibration Co., Ltd. [28].

To measure the screen luminance, we enclosed the lens and light meter's photo sensor dome with a truncated cone that was cut in half longitudinally. The cone was coated with Black 3.0, a non-reflective color, from Stuart Semple's studio to reduce reflectance from within and outside the cone [29], [30]. The distance between the LCD screen and the lens was 63 millimeters (mm), which is within the minimum and maximum focal length of the lens. In addition, the distance between the lens and photo sensor dome was approximately 15 mm, which was similar to the distance between the lens and subject's eye in our GlauCUTU VR device.

Luminance of display screen was quantified by initially measuring the lowest light step level and increasing the light step level by increments of 5 steps of Red, Green, and Blue (RGB) using our Python code on library OpenCV 0.4.3.

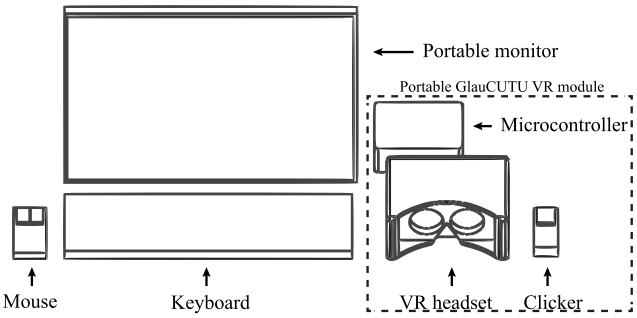

FIGURE 2. GlauCUTU perimetry set up composing of the portable GlauCUTU VR module, a display screen, keyboard, and mouse set.

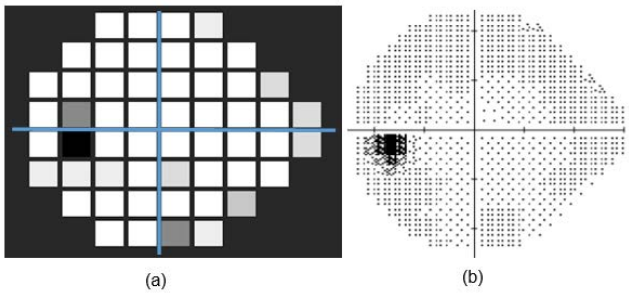

FIGURE 3. Example of visual field mapping between (a) preliminary GlauCUTU test result vs. (b) HFA result from the same subject.

The display screen had a luminance range between 0 light step level (black, 0 lux) and 255 light step level (white, 133.3 lux). The direct correlation between light step level and luminance is illustrated in Fig. 1.

The proposed module composes of a VR headset, an NVIDIA® Jetson Nano microcontroller, and a clicker. For the perimetry test, we used a screen display size 15.6'', a keyboard, a mouse set, a signal cable, and a power adaptor along with the portable GlauCUTU VR set as shown in Fig. 2. The clicker weighs around 40 grams and can be held comfortably with indentations designed for finger engagement. The VR headset is lightweight at approximately 350 grams and can be tightly mounted with the adjustable straps to appropriately fit each subject's head. The total weight of the portable VR module is around 390 grams. The test reports real-time results including fixation loss and false positive rate, as well as parameters such as stimulus presentation rate. Our VR perimetry test is easy to be set up and ready to use within 3 minutes.

B. SOFTWARE FEATURES

Jetson Nano utilizes the JetPack 4.5.1 based on Ubuntu, which enables the development of an automated perimetry system. The perimetry test was mainly controlled by the conventional Python 3.6.0 and OpenCV 3.4.2 to provide rapid updates and improvements. In our preliminary study, GlauCUTU test utilized the modified bracketing method with three levels of stimulus intensity: low, moderate, and high light levels or equivalent to GlauCUTU sensitivities of 16.2, 11.95, and 1.5 dB, respectively. The participants were instructed to focus on the fixation marker at the center of the VF throughout the test and to immediately press the clicker once they perceived the stimulus.

The algorithm began with a stimulus of moderate light intensity and once the participant responded to the stimulus, it will decrease to low intensity. On the other hand, if there was no response to moderate light intensity, a stimulus of high intensity will be examined at the same location. Fig. 3a shows an example of our preliminary GlauCUTU test results. Darker color represents that a higher level of stimulus intensity was required for participant to detect the stimulus. This preliminary test showed that our VR headset could be used for measuring different contrast sensitivities and detecting visual field defects.

As perimetry test requires participants to fixate their eye on the fixation marker, long test time induces eye fatigue and reduces test reliability [31]. To reduce test time for both eyes, GlauCUTU utilized an ascending method of limits — the study in which stimulus is presented initially at a low light intensity and gradually increases in intensity until the participant perceives it — to measure a participant's perception of the stimulus [20]. Moreover, the stimulus size in GlauCUTU differs from HFA as GlauCUTU employed the spatially equated stimulus map with stimulus size of Goldmann I, II and III target sizes [32].

Different target sizes with diameters of 0.2, 0.32, and 0.5 degrees were used across the VF. The stimulus increased in size as its location moves from central to peripheral. The spatially equated stimulus map, which uses stimulus sizes that are within or near the critical area of spatial summation of healthy subjects, has been shown to help detect glaucoma in its earlier stages [33]. The fixation marker in GlauCUTU, a green disc with diameter of 0.65 degree, remained the same for all tests. GlauCUTU used a moving fixation marker to enhance participant's attention and expand the VF range.

GlauCUTU used the 24-2 test pattern, with examination of 54 points that were 6° apart and 12 points were located in the central 10° of fixation [8], [34], [35]. The parameters within the GlauCUTU program can be adjusted for different types of screening such as amblyopia, but this study will focus on glaucoma screening. Adjustable parameters included stimulus presentation time, range of stimulus intensity, and background intensity to make the test suitable for each subject. Stimulus presentation rate can be adjusted to allow time for participant to focus on the target.

In this study, the background luminance was set to 30 light step level. The range of stimulus luminance was between 30 light step level (20.26 dB) and 235 light step level (0 dB). Stimulus intensity was increased by increments of 150 light step level per second. Once the parameters were selected, the examiner informed participants to fix their eyes on the fixation marker at the center of the VF throughout the calibration process and perimetry test. Display screen settings were calibrated by displaying the stimuli at all tested 54 VF

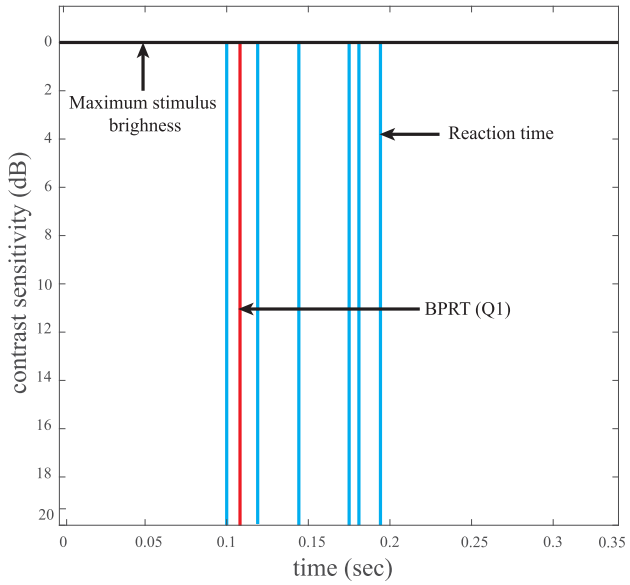

FIGURE 4. Example of pretest analysis which collected 6 RTs to obtain BPRT.

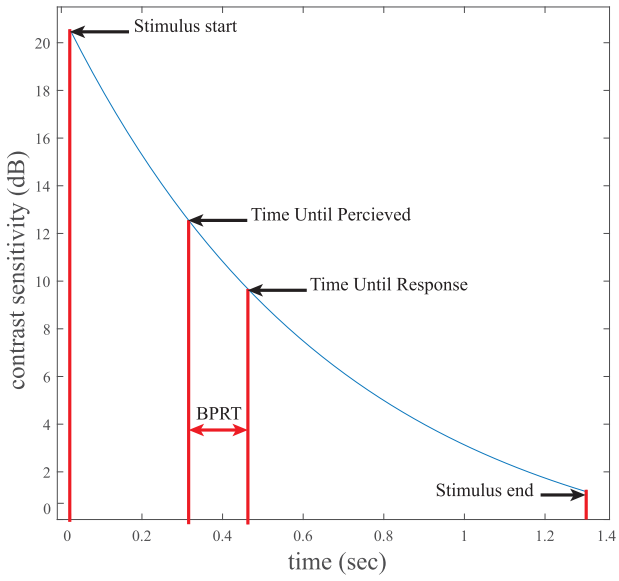

FIGURE 5. The relationship between BPRT, TUR, and TUP.

locations for both eyes simultaneously. Then, the examiner asked the participant to describe characteristics of the points and quality of image displayed on screen to confirm that all tested VF locations were within field of view.

After configuration of appropriate parameters, the examiner manually identified the participant's blind spots by simultaneously relocating the two red disc stimuli until they disappeared. The blind spots were initially inferred to be at 15° temporal to the fixation marker in the VF according to the physiologic blind spot [12]. Once both blind spots were detected, the examiner informed participants to immediately respond to a white disc stimulus (the spatially equated stimulus) displayed on the LCD screen by pressing the clicker.

Each subject underwent a pretest which involved projecting the brightest stimulus at four different locations that are 5° in the nasal, temporal, superior, and inferior direction from the fixation marker. The stimulus was projected twice at each location for both eyes. RT — the duration the participant takes to respond to the brightest stimulus —of each location was collected. The pretest was completed after the participant responded to at least 6 projected stimuli. Best possible reaction time (BPRT) was calculated from values in the first quartile among collected RTs during the pretest as shown in Fig. 4. BPRT represents the participant's and system's latency that occurs after the participant perceives the stimulus.

In the GlauCUTU perimetry test, all 54 tested VF locations were tested in a random order. The stimulus was presented once at each tested VF location. Both eyes were projected with the stimulus in alternating order. At each tested VF location, the stimulus gradually increased in intensity from 30 to 235 light step level until the participant responded to the stimulus. TUR was collected once the participant responded to the stimulus by pressing the clicker.

During the test, the stimulus was repeatedly presented at the blind spot approximately every 10 clicks to evaluate fixation loss. Moreover, latency analysis was assessed every 25 clicks to detect false positive responses. Latency analysis proposes the same process as the pretest but only requires responses to at least 3 projected stimuli. After each latency analysis, new collected data will be included with previous latency analysis and pretest results to calibrate participant's BPRT. BPRT was used as a reliability index for evaluation of false positive results. False positive results were indicated in circumstances where TUR is more than 20% faster than BPRT. Tested locations with false positive responses were regarded as suspicious points and retested to increase result accuracy and reliability.

III. AUTOMATED TRANSFORMATION DESIGN

To determine GlauCUTU sensitivity, we estimated TUP — the time interval starting from presenting stimulus with lowest luminance until the participant perceives it — by factoring out BPRT from TUR as illustrated in Fig. 5 and calculated by Eq. 1. GlauCUTU sensitivity was estimated from TUP using the exponential Eq. 2, which is depicted as a curve-fitting non-linear line in Fig. 6. The negative correlation between TUP and GlauCUTU sensitivity in Fig. 6 demonstrates that the longer the TUP, the lower the sensitivity. The highest difference in sensitivity is between TUP of 0–0.4 seconds signifying that a small change in TUP of 0–0.4 seconds is sensitive in detecting a drop in GlauCUTU sensitivity levels.

$$TUP = TUR - BPRT, \tag{1}$$

where, TUP is time until perceived. TUR is time until response and $BPRT$ is the best possible reaction time.

$$\hat{E}_{\mathrm{dB}} = 23.375 \times e^{-1.3838 \times \mathrm{TUP}} - 3.162, \tag{2}$$

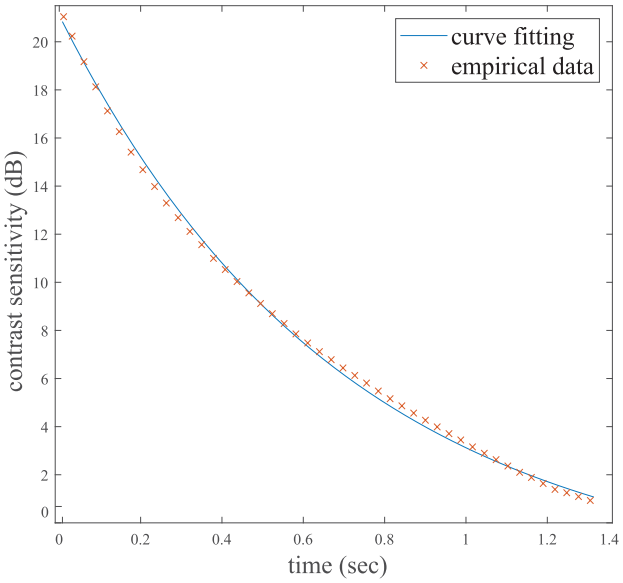

FIGURE 6. The relationship between GlauCUTU sensitivity in dB (y-axis) and time in seconds (x-axis) with a curve fitting derived from empirical data.

where $\hat{E}_{\text{dB}}$ is an estimation of GlauCUTU sensitivity and TUP is time until perceived.

GlauCUTU used an RGB scale for display adjustment, which corresponds to screen luminance using Fig. 1. Stimulus brightness ranged from 30−235 light step level or 1.02−108.30 lux to evaluate GlauCUTU sensitivity of 0−20.26 dB. While in HFA, stimulus brightness ranged from 0.10 to more than 10,000 apostilb (asb) or equivalent to HFA sensitivity of between 0−50 dB. Differences between GlauCUTU and HFA sensitivities challenge direct comparison between the two tests. Hence, GlauCUTU sensitivity was used to estimate HFA sensitivity for each stimulus brightness using automated transformation algorithms.

We developed algorithms for transforming GlauCUTU sensitivity map into HFA sensitivity map. The proposed study compares the performances of selective ML algorithms such as Locally Weighted Learning (LWL), Multi-layer Perceptron (MLP), Additive Regression (AddReg), Reduced Error Pruning Tree (REPTree), Voter [36], [37], and DL algorithm-based ResNet [38]. All of the proposed algorithms employed the same leave-one-subject-out cross-validation to predict model performance of the testing data. One subject was randomly selected to validate the model's predictive performance and the subject's information will be excluded from training to prevent bias.

Performances of several ML and DL methods were compared for selection of the highest performing method to create the novel automated transformation algorithm. The Weka tool [39], a data mining software, was used to assess performances of ML algorithms. The kernel size 3 × 3 with zero padding of untested locations was applied to incorporate neighboring points as the input to reduce fluctuation in GlauCUTU sensitivity by providing more information [40].

Our augmentation method was based on the work of Ferreras *et al.* about mapping visual field to corresponding retinal nerve fiber layers [41]. Our study proposes overlapping of two visual fields from different subjects to synthesize new training dataset as depicted in Fig. 7. Unlike most pre-trained model, custom deep neural network enables adjustment of input size and network architecture so we employed ResNet architecture with residual block, which uses skip-connections to reduce redundant layers and mitigate vanishing gradient and degradation problems. Skip-connections enable training of deeper networks by providing identity functions and ensuring that initial layers are as efficient as the final layers [38].

Moreover, we also incorporated an autoencoder model [42] into the trained network. The autoencoder is an unsupervised learning technique that consists of two networks, encoder and decoder. Encoder compressed the input to extract meaningful information, which was then reconstructed by the decoder as the output for robust predictions [43]. In our network, the input was a 24–2 visual field map plotted on a [10 × 10] square matrix. The upsampling layer turned the input into a [20 × 20] square matrix, which later underwent three layers of residual blocks for information extraction and two layers of residual blocks for decompressing to create a visual field map. As the network was trained from scratch with a dropout rate of 0.5, weight initialization was completed using He initialization [44] and Adamax algorithm for optimization of parameters during training process [45].

Modified Mean Absolute Percentage Error (MMAPE) is a loss function to evaluate the network's performance. Loss function determines the absolute percentage difference between HFA threshold and prediction threshold to evaluate and improve network's performance. Mean Absolute Percentage Error (MAPE) was initially applied on DL but was limited by zero division in VF locations that did not incite any response. To avoid zero division error, we used the MMAPE by adding a constant to the loss function as shown in Eq. 4. Based on our experiments, initialization of C with 12.5 dB greatly improved prediction accuracy.

$$\text{MMAPE} = \frac{100}{n}\sum_{t=1}^{n}\left|\frac{(A_t + C) - (F_t + C)}{A_t + C}\right| \tag{3}$$

$$= \frac{100}{n}\sum_{t=1}^{n}\left|\frac{A_t - F_t}{A_t + C}\right|, \tag{4}$$

where A_t is the actual value. F_t is a forecast value and C is a constant of 0.3.

IV. EXPERIMENTAL DESIGN AND SETUP

This section includes details regarding the study group enrolled in this study and the development process of GlauCUTU VR perimetry including both hardware and software features and the experimental process.

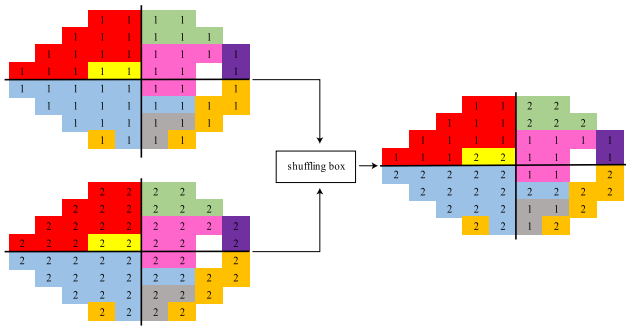

FIGURE 7. Visual field mappings from two eyes are combined at random for data augmentation. The two numbers represent each subject's visual field. The colors indicate correlated visual field areas for diseases of the optic nerve (modified from Ferreras *et al.* [41]).

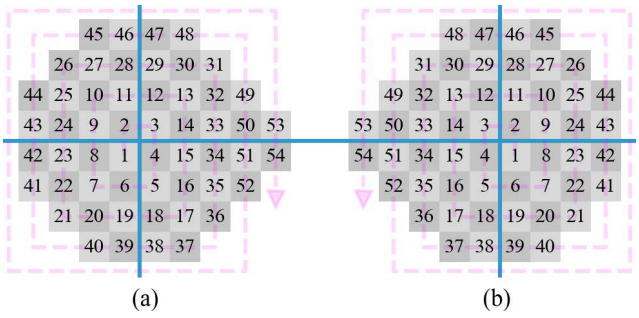

FIGURE 8. GlauCUTU visual mapping of a) OS configuration and b) OD configuration. The arrow represents ranking of visual field location from 1 to 54.

A. STUDY GROUP

The protocol for this study was approved by the Chulalongkorn Institutional Review Board (No. 715/61) and all subjects signed informed consent statements. Patients who attended King Chulalongkorn Memorial Hospital's out-patient ophthalmology clinic underwent prospective evaluation. Subjects were selected and invited to participate according to their medical records. A total of 31 subjects were enrolled in the study providing 62 eyes of which 16 eyes are from 8 glaucoma patients, 4 males and 4 females, with an average age of 67.75±7.30 years. The glaucomatous eyes were classified based on severity: 7 eyes with early glaucoma defect, 3 eyes with moderate defect, and 6 eyes with severe defect. The control group includes 46 eyes from 23 non-glaucoma patients with an average age of 46.16±15.07 years. The normal subjects' eyes were classified as 45 normal eyes and 1 eye with early glaucoma defect.

The inclusion criteria were 18 years of age or older, no known history or clinical manifestations of neurological or psychological disorders, and having best reported visual acuity (VA) of 20/70 or better. The inclusion criteria for the glaucoma study group was having a diagnosis of primary glaucoma according to the Hodapp-Parrish-Anderson (HPA) criteria along with visual field defects detected by SAP (HFA, Carl Zeiss Meditec, Dublin, CA) within the past 3 months [10], [46]. The inclusion criteria for the control group was having normal intraocular pressure and no evidence of glaucomatous optic neuropathy with normal visual field reported by SAP according to HPA criteria within the past 3 months [46]. The exclusion criteria included subjects with other non-glaucomatous diseases that can cause visual field defects and those receiving medications that affect the nervous system such as haloperidol and diazepam.

B. EXAMINATION PROCEDURE

Each participant underwent the standard HFA and the GlauCUTU test at least 30 minutes apart in random order within the same day. Both GlauCUTU and HFA were tested using the 24-2 test pattern. The HFA test was executed based on standard protocol, while the GlauCUTU test was performed as follows. The VF test composing of a VR headset, a clicker, a Jetson Nano microcontroller, a portable monitor, a mouse and keyboard, a signal cable, and a power adaptor was configured. The subject underwent history taking for information pertinent to the study and his or her pupillary distance was measured.

The VR headset was positioned appropriately to avoid LRA and was adjusted to match the subject's pupillary distance. Subjects were allowed to wear their own glasses underneath the VR headset for refractive correction. Software parameters such as background luminance, stimulus presentation time, and fixation errors can be selected from available presets or customized. Blind spot was manually detected followed by the pretest. Then, the actual test using the 24-2 test pattern commenced with latency analysis occurring every 25 responses. Once all the assigned points have been tested, the software analyzed the results and generated an electronic report.

The report includes fixation error, false positive rate, and the participant's visual field pattern similar to HFA, based on the visual mapping depicted in Fig. 8. If those values were higher than the accepted values, the participant was required to repeat the test after a 15-minute break. HFA sensitivity derived from GlauCUTU-ML and GlauCUTU-DL for comparison were then used to determine the VFI for glaucoma severity classification as depicted in Fig. 9.

The duration of the GlauCUTU VF test was approximately 7–9 minutes and included pupillary distance set up, manual blind spot localization, pretest and latency analysis, and the actual test. Eye fixation lasted 6–8 minutes, which included blind spot detection, pretest and latency analysis and the actual test. Meanwhile, the duration of the actual HFA test excluding set-up time was around 10 minutes. We can only conclude that GlauCUTU test entails shorter duration that requires eye fixation. GlauCUTU test time which includes the pretest, latency analysis, and the actual test amounts to an average of less than 290 seconds for both eyes when compared to the average HFA test time of 600 seconds for both eyes.

Longer test duration can cause test-induced eye fatigue which may lead to lower threshold values and reduced test

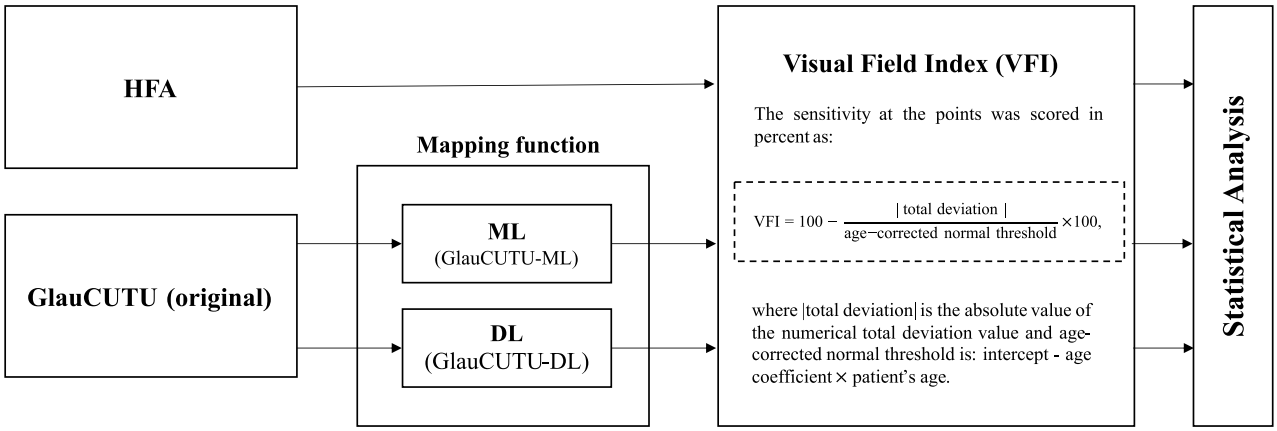

FIGURE 9. Flow diagram of the proposed study on GlauCUTU VF analyzer which collects GlauCUTU sensitivities to compare with HFA results. For each of 54 VF test points, GlauCUTU-original estimated HFA sensitivity (dB) using ML and DL mapping functions. Then, VFI of each eye was calculated based on the 54 estimated HFA sensitivities. The estimated VFI-based GlauCUTU-ML and GlauCUTU-DL were compared to VFI of HFA using statistical analysis.

reliability [31]. The test time varies for each participant. Duration is lengthened in cases with many defective points that are inconsistent with BPRT that require more retests on the suspicious points. A longer test time can either reflect visual field defects or slower response to the stimulus. The duration of each subject's visual fixation was compensated by adjusting stimulus presentation time to allow more time for the eyes to align with the new target.

C. INTER-RATER RELIABILITY AND TEST VALIDITY

VF results from GlauCUTU-original, GlauCUTU-ML, and GlauCUTU-DL were compared to those of HFA by three expert ophthalmologists. Agreement between HFA and GlauCUTU VF tests indicates correspondence between at least two out of three raters. Percentage of agreement and Gwet's AC1 coefficient was calculated to assess validity of GlauCUTU tests in comparison to HFA. In addition, VF test validity was evaluated by comparing between the raters' gradings of HFA to GlauCUTU-original, GlauCUTU-ML, and GlauCUTU-DL.

V. EXPERIMENTAL RESULTS

A. OBJECTIVE RESULTS

In Fig. 10, non-glaucomatous eyes have high HFA sensitivities denoted by the whiter shades. As GlauCUTU and HFA utilize different target sizes [33], GlauCUTU-original's Hill of Vision presents a different shape from HFA's Hill of Vision [33]. These findings cannot be directly compared to HFA results. Hence, the difference between HFA and GlauCUTU necessitates an automated transformation from GlauCUTU sensitivity to HFA sensitivity. GlauCUTU-ML's Hill of Vision and GlauCUTU-DL's Hill of Vision are similar to HFA's Hill of Vision as sensitivities are decreased at peripheral VF locations.

Objective evaluations of automated transformation algorithms and HFA include mean absolute error (MAE), RMSE, Pearson's r correlation coefficient, and VFI. MAE and RMSE represent deviation from the HFA sensitivity, but RMSE is more influenced by outliers. GlauCUTU-ML algorithms included LWL, MLP, AddReg, REPTree, and Voter. While, GlauCUTU-DL was ResNet. LWL, MLP, AddReg, REPTree, Voter, and ResNet were evaluated for the development of the automated glaucoma severity prediction, which predicts HFA sensitivities from VFI of GlauCUTU sensitivity.

Pearson's r correlation coefficients ranked from highest to lowest were as follows: ResNet, AddReg, LWL, Voter, REPTree, and MLP with values of 0.74±0.23, 0.70±0.17, 0.69±0.18, 0.66±0.19, 0.55±0.24, and 0.53±0.27, respectively. RMSE from lowest to highest is LWL, AddReg, Voter, REPTree, MLP, and ResNet with 4.92±2.18, 5.16±1.45, 5.37±2.20, 5.70±2.44, 5.99±3.14 and 6.31±1.30, respectively. MAE from lowest to highest is LWL, AddReg, MLP, Voter, REPTree, and ResNet with 3.50±1.66, 3.50±1.17, 3.76±2.19, 3.80±1.76, 3.80±1.73 and 3.88±0.77, respectively.

Although the deep-learning ResNet method has the best performance with the highest Pearson's r correlation coefficients of 0.74, it also has the highest MAE and RMSE of 3.88 and 6.31, respectively as shown in Table 1. Among all algorithms, LWL produces the most promising results with a Pearson's r correlation coefficient of 0.69 and the lowest RMSE and MAE values of 4.92 and 3.50, respectively. MLP and REPtree have similar results with average Pearson's r correlation coefficient with SD of 0.53±0.27 and 0.55±0.24, respectively. With the decision tree method, AddReg has a better overall performance when compared to REPTree with Pearson's r coefficient 0.70 and 0.55, respectively.

Voter, which aggregates results of multiple ML methods, yields MAE and Pearson's r correlation coefficient of 3.80±1.76 and 0.66±0.19, respectively. In Fig. 11, AddReg and ResNet produce similar MAE trend lines indicating that the average difference between the predicted and HFA

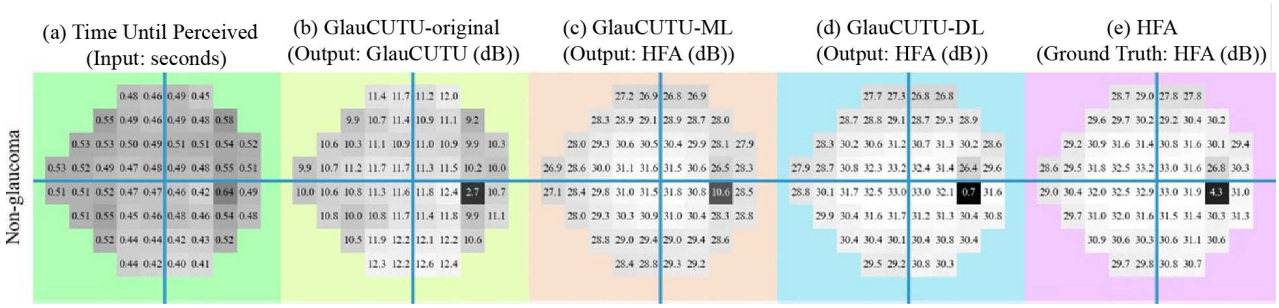

FIGURE 10. Grayscale mapping of non-glaucoma subjects evaluated using a) time until perceived, b) GlauCUTU-original, c) GlauCUTU-ML, d) GlauCUTU-DL and e) HFA. Average time until perceived from shortest to longest is shown in lightest to darkest tone, respectively. Average sensitivities from lowest to the highest are represented by darkest to lightest tone, respectively, in columns b, c, d and e. Column b is reported in GlauCUTU sensitivity (dB), while columns c, d and e are reported in HFA sensitivity (dB).

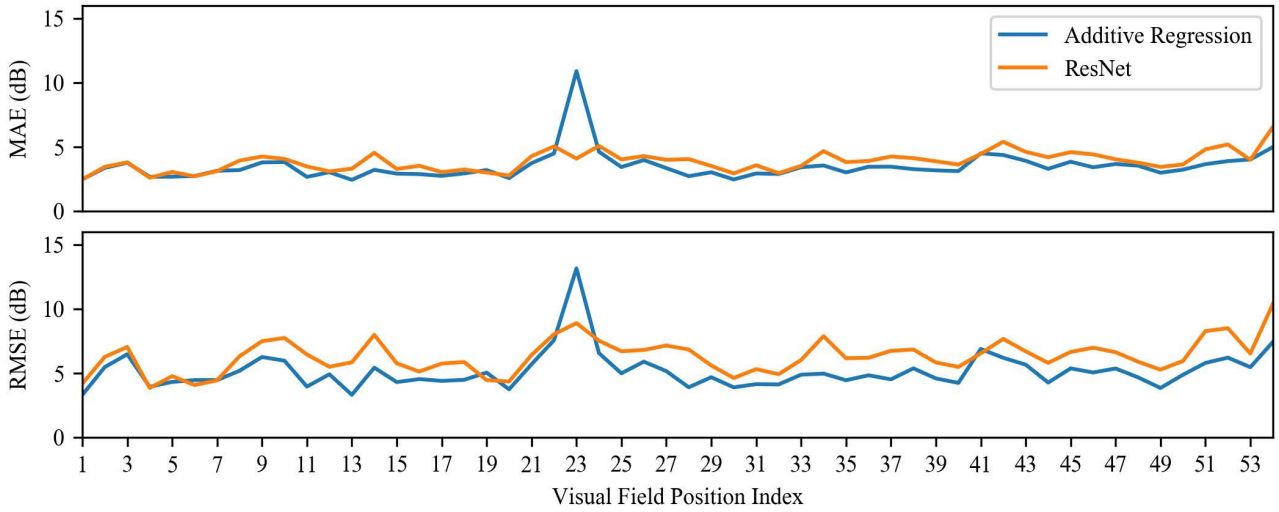

FIGURE 11. Presentations of MAE and RMSE values of two automated transformation algorithms compared to HFA at 54 VF positions. Automated transformation algorithms, AddReg and ResNet, are portrayed in blue and orange lines, respectively.

TABLE 1. MAE, RMSE, and Pearson's *r* correlation coefficient results of different algorithms for conversion between GlauCUTU sensitivity and HFA sensitivity.

Method	MAE± SD (dB)	RMSE± SD (dB)	Pearson's r± SD
LWL	3.50±1.66	4.92±2.18	0.69±0.18
MLP	3.76±2.19	5.99±3.14	0.53±0.27
AddReg	3.50±1.17	5.16±1.45	0.70±0.17
REPTree	3.80±1.73	5.70±2.44	0.55±0.24
Voter	3.80±1.76	5.37±2.20	0.66±0.19
ResNet	3.88±0.77	6.31±1.30	0.74±0.23

sensitivity is around 3 dB. ResNet has higher RMSE values indicating that it produces more outliers. AddReg has the highest MAE and RMSE at VFI of 23, which is the physiologic blindspot.

The results of visual field mapping from GlauCUTU, GlauCUTU with automated transformations, and HFA are shown in Fig. 12. AddReg has been selected for GlauCUTU-ML and ResNet is representative of GlauCUTU-DL. GlauCUTU-ML and GlauCUTU-DL produce the closest results to those of HFA in non-glaucomatous and early glaucomatous eyes shown in rows 1 and 2 of Fig. 12. For moderate glaucoma, GlauCUTU-original and GlauCUTU-ML produce visual field mappings similar to HFA, as depicted in row 3 of Fig. 12. As for severe glaucoma shown in row 4 of Fig. 12, GlauCUTU-DL produces a grayscale mapping with the most similar visual field defect pattern to HFA. GlauCUTU-original generates more VF defects in the lower quadrants and GlauCUTU-ML underestimates the defective locations. In column (a) of Fig. 12, there is an increasing trend in TUP from normal to severe glaucoma.

The comparisons between HFA, GlauCUTU-ML, and GlauCUTU-DL were examined using VFI, which evaluates percentage of visual function [47]. The statistical analysis reveals that there are no significant difference between the VFI of GlauCUTU-ML and GlauCUTU-DL with HFA for the entire dataset (p=0.996 for HFA vs. GlauCUTU-ML and p=0.805 for HFA vs. GlauCUTU-DL). Similarly, there are no significant differences between VFI of GlauCUTU with automated transformations and HFA in normal controls (p=0.999 for HFA vs. GlauCUTU-ML and p=0.977 for HFA vs. GlauCUTU-DL) as well as in patients with early (p=0.999 for HFA vs. GlauCUTU-ML

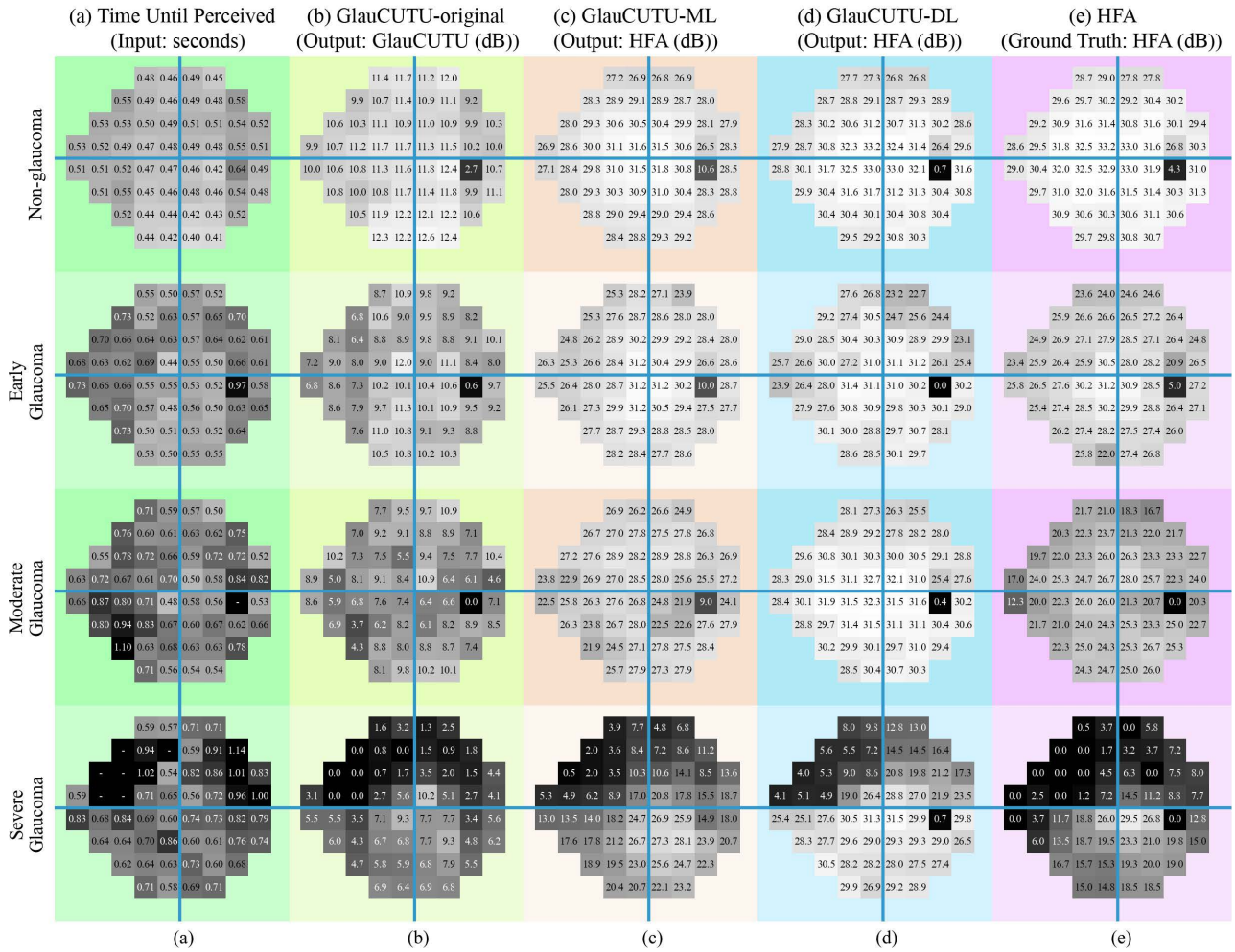

FIGURE 12. Comparison of HFA sensitivity and grayscale mapping of a) time until perceived, b) GlauCUTU-original, c) GlauCUTU-ML, d) GlauCUTU-DL and e) HFA results collected from randomly selected participants' eyes. Visual field mappings from each algorithm of non-glaucoma, early glaucoma, moderate glaucoma, and severe glaucoma eyes from each algorithm are compared from the top to bottom row, respectively. Column b is reported in GlauCUTU sensitivity, while columns c, d and e are reported in HFA sensitivity. In columns b, c, d and e, sensitivities from lowest to the highest are represented by darkest to lightest tone, respectively. In column a, duration from shortest to longest is shown from lightest to darkest tone, respectively.

and p=0.999 for HFA vs. GlauCUTU-DL) and moderate glaucoma (p=0.997 for HFA vs. GlauCUTU-ML and p=1.000 for HFA vs. GlauCUTU-DL). Similarly, there is no significant difference between HFA and GlauCUTU-ML in severe glaucoma (p=0.573). The only significant difference reported in our study is the post-hoc analysis between GlauCUTU-DL and HFA when tested on subjects with severe glaucoma ($p<0.05$) as shown in Fig. 13.

B. SUBJECTIVE RESULTS

Subjective evaluation of GlauCUTU was examined using majority voting agreement by clinicians and inter-rater reliability between HFA, GlauCUTU-original, GlauCUTU-ML, and GlauCUTU-DL. Validity of subjective ratings was based on clinical judgement of the pattern and location of VF defects. Upon comparing each pair of VF mappings, the ophthalmologists determined whether they were identical.

TABLE 2. Percentage agreement of the majority vote of GlauCUTU-original, GlauCUTU-ML, and GlauCUTU-DL compared to HFA are depicted according to glaucoma severity.

	HFA & GlauCUTU-original	HFA & GlauCUTU-ML	HFA & GlauCUTU-DL
Normal	0.200	0.875	0.429
Early glaucoma	0.500	1.000	0.333
Moderate glaucoma	0.667	0.778	0.800
Severe glaucoma	0.500	0.667	0.333

Clinicians' majority voting agreement was done using the percentage of agreement from at least two of three ophthalmologists. While, inter-rater reliability was assessed by three expert ophthalmologists who compared results from HFA to those of GlauCUTU-original, GlauCUTU-ML, and GlauCUTU-DL.

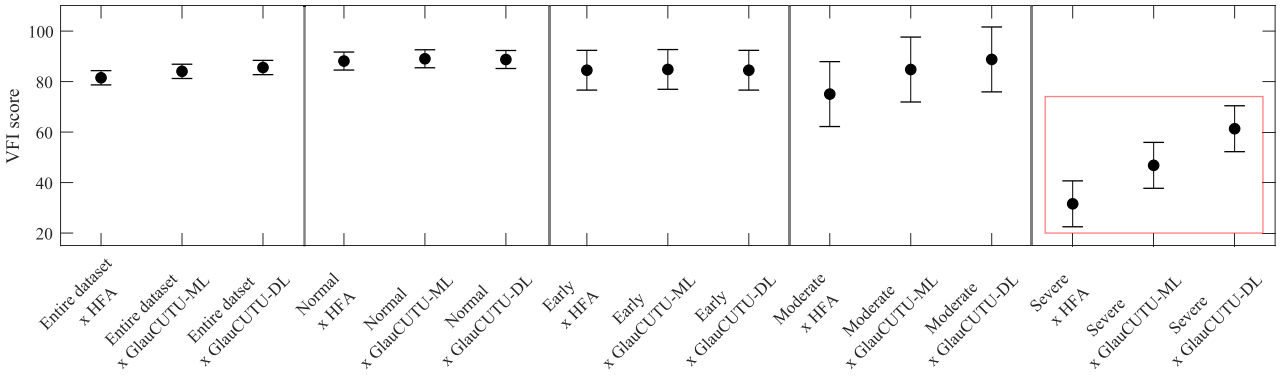

FIGURE 13. Post-hoc analysis of two-way ANOVA between the factor of scheme (x-axis) and VFI (y-axis) for the performances of HFA, GlauCUTU-ML,and GlauCUTU-DL on the entire, early glaucoma, moderate glaucoma, and severe glaucoma datasets.

The VF images from GlauCUTU-original, GlauCUTU-ML, and GlauCUTU-DL were initially rated by three ophthalmologists. Each ophthalmologist was asked to confirm the validity between HFA and GlauCUTU's VF. Any of GlauCUTU's VF with at least two confirmed validity was considered as an agreement to HFA. Table 2. shows the percentage of agreement between HFA and GlauCUTU-original, GlauCUTU-ML, and GlauCUTU-DL for different glaucoma severity. The results indicated that GlauCUTU-original has the poorest performance, as per our assumption. The GlauCUTU-ML yields the best performance by increasing the percentage of agreement when compared to GlauCUTU-original by 0.675, 0.500, 0.111, and 0.167 in normal eyes, the early glaucoma group, moderate glaucoma subjects, and the severe glaucoma group, respectively, as calculated from columns 1 and 2 of Table 2.

Meanwhile, when compared to GlauCUTU-original, GlauCUTU-DL only increases the percentage of agreement in the normal and moderate glaucoma group by 0.229 and 0.133, respectively, while decreasing in performance for early and severe glaucoma by 0.167 and 0.167, respectively, depicted in columns 1 and 3 in Table 2. Reliability analysis of each algorithm was based on comparison of inter-rater reliability between HFA and GlauCUTU-original, GlauCUTU-ML and GlauCUTU-DL. The Gwet's AC1 coefficient of GlauCUTU-original, GlauCUTU-ML, and GlauCUTU-DL are 0.481, 0.546, and 0.532, respectively, which demonstrates that GlauCUTU-ML had the highest performance. The results of post-hoc and reliability analysis conclude that GlauCUTU-ML achieved the greatest performance, followed by GlauCUTU-DL and lastly GlauCUTU-original.

Reliability analysis of each algorithm was based on comparison of inter-rater reliability between HFA and GlauCUTU-original, GlauCUTU-ML, and GlauCUTU-DL. The Gwet's AC1 coefficient of GlauCUTU-original, GlauCUTU-ML, and GlauCUTU-DL are 0.481, 0.546, and 0.532, respectively, which confirms that GlauCUTU-ML had the highest performance [48]. The results of post-hoc and reliability analysis conclude that GlauCUTU-ML achieved the greatest performance, followed by GlauCUTU-DL then GlauCUTU-original.

VI. DISCUSSION AND FUTURE WORK

In our previous work, GlauCUTU results demonstrated a prolonged mean TUR in the glaucoma group when compared to the control group [20]. As an extension, this work successfully developed GlauCUTU, a TUP-based perimetry tool, for glaucoma screening and classification of glaucoma severity. GlauCUTU produces results clinically comparable to HFA using our novel automated transformation, which enables conversion of GlauCUTU sensitivity into HFA sensitivity. The predicted sensitivity mappings from GlauCUTU-ML and GlauCUTU-DL produce promising patterns that are similar to HFA.

GlauCUTU's performance was compared to HFA using objective evaluations of MAE, RMSE, Pearson's r correlation coefficient, and VFI. GlauCUTU-ML using AddReg produces the lowest MAE. GlauCUTU-DL trained with synthetic data has the highest MAE, which may be due to test-retest variability. ResNet classifier yields the highest Pearson's r correlation coefficient indicating its high prediction performance. ResNet also has the highest RMSE indicating that predictions from ResNet provide the most outliers to the ground truth which may be attributed to the augmentation method.

According to Fig. 11, the 23rd visual field location represents the most common physiologic blind spot, in which ResNet presents more information on that location than AddReg. This property of ResNet can be attributed to the network's considerable amount of parameters, which enhances its ability to recognize the blind spot along with determining the frequency of that location. Although both ResNet and AddReg produce similar MAE values, ResNet creates more outliers in the visual map, as seen in Fig. 11. Meanwhile, AddReg produces more accurate predictions. Furthermore, the mapping of sensitivity to VFI function for GlauCUTU-ML with no significant differences between each glaucoma severity support the use of GlauCUTU-ML's for transforming GlauCUTU sensitivity into HFA sensitivity.

Subjective evaluations of clinicians' majority vote agreement and inter-rater reliability was used to compare between GlauCUTU and HFA. The subjective evaluations demonstrated high reliability agreement with clinician's

interpretation of HFA results. Furthermore, GlauCUTU's average test duration is lower than HFA as it uses the ascending methods of limit to evaluate contrast sensitivity and also evaluates BPRT. By calculating each participant's BPRT, the system can appropriately select specific retest locations (locations with false positive result). Shortened test time help decreases test-induced eye fatigue leading to more reliable results [31].

The head-mounted VR device provides a portable and comfortable alternative to the HFA [7], [13], [14]. Moreover, GlauCUTU is an affordable perimetry system which can be implemented in low-resource areas such as in rural hospitals. GlauCUTU costs less than 1,000 USD, as opposed to the 40,000 USD price tag for the HFA device. One limitation in our current version of GlauCUTU is that it requires manual work from a trained technician during the calibration process.

With many advantages, GlauCUTU and the novel automated transformation, can potentially increase accessibility to accurate glaucoma screening in rural areas. This novel perimetry system will be beneficial to both the healthcare system and the patients by serving as an applicable and affordable screening tool for glaucoma to prevent delayed diagnosis and treatment. The portable VF test can be implemented anywhere making perimetry tests accessible even for users under home isolation during the global pandemic. In the future, we plan to recruit more participants for this study to improve the prediction performance of our automated transformation technology. We aim to integrate the head-mounted VR perimetry along with the novel automated transformation AI with our optic disc and cup segmentation network model for glaucoma detection. All in all, our ultimate goal is to reduce irreversible blindness from glaucoma by enhancing accessibility to glaucoma screening in low resource countries such as Thailand.

ACKNOWLEDGMENT

The authors would like to thank Wisaruta Wutthayakorn, M.D., Nopphawan Uramphorn, M.D., Patcharaporn Jaru-Ampornpan, M.D., Natnaree Taechajongjintana, M.D., Pattawee Pongpisitkul, M.D., Pukkapol Suvannachart, M.D., and Aim-On Saengsirinavin, M.D., from the Faculty of Medicine, Chulalongkorn University for their contributions.

REFERENCES

[1] D. H. Johnson, "Progress in glaucoma: Early detection, new treatments, less blindness," *Ophthalmology*, vol. 110, no. 4, pp. 634–635, Apr. 2003.
[2] A. L. Coleman and S. Miglior, "Risk factors for glaucoma onset and progression," *Surv. Ophthalmol.*, vol. 53, no. 6, pp. S3–S10, Nov. 2008.
[3] Y.-C. Tham, X. Li, T. Y. Wong, H. A. Quigley, T. Aung, and C.-Y. Cheng, "Global prevalence of glaucoma and projections of glaucoma burden through 2040: A systematic review and meta-analysis," *Ophthalmology*, vol. 121, no. 11, pp. 2081–2090, 2014.
[4] C. B. Estopinal, S. Ausayakhun, C. Jirawison, T. P. Margolis, and J. D. Keenan, "Access to ophthalmologists in Thailand: A district-level analysis," *Invest. Ophthalmol. Vis. Sci.*, vol. 53, no. 14, p. 1422, 2012.
[5] G. Michelson and M. J. M. Groh, "Screening models for glaucoma," *Current Opinion Ophthalmol.*, vol. 12, no. 2, pp. 105–111, Apr. 2001.
[6] D. C. Broadway, "Visual field testing for glaucoma—A practical guide," *Community Eye Health*, vol. 25, nos. 79–80, pp. 66–70, 2012.
[7] D. Wroblewski, B. A. Francis, A. Sadun, G. Vakili, and V. Chopra, "Testing of visual field with virtual reality goggles in manual and visual grasp modes," *BioMed Res. Int.*, vol. 2014, pp. 1–10, Jun. 2014.
[8] L. Mees, S. Upadhyaya, P. Kumar, S. Kotawala, S. Haran, S. Rajasekar, D. S. Friedman, and R. Venkatesh, "Validation of a head-mounted virtual reality visual field screening device," *J. Glaucoma*, vol. 29, no. 2, pp. 86–91, 2020.
[9] S. L. Pineles, N. J. Volpe, E. Miller-Ellis, S. L. Galetta, P. S. Sankar, K. S. Shindler, and M. G. Maguire, "Automated combined kinetic and static perimetry: An alternative to standard perimetry in patients with neuro-ophthalmic disease and glaucoma," *Arch. Ophthalmol.*, vol. 124, no. 3, pp. 363–369, 2006.
[10] A. Heijl, "The Humphrey field analyzer, construction and concepts," in *Proc. 6th Int. Vis. Field Symp.*, Dordrecht, The Netherlands, 1985, pp. 77–84.
[11] D. R. Anderson and V. M. Patella, *Automated Static Perimetry*. St. Louis, MO, USA: Mosby Year Book, 1992.
[12] D. A. Hollander, N. J. Volpe, M. L. Moster, G. T. Liu, L. J. Balcer, K. D. Judy, and S. L. Galetta, "Use of a portable head mounted perimetry system to assess bedside visual fields," *Brit. J. Ophthalmol.*, vol. 84, no. 10, pp. 1185–1190, Oct. 2000.
[13] S. Tsapakis, D. Papaconstantinou, A. Diagourtas, K. Droutsas, K. Andreanos, M. M. Moschos, and D. Brouzas, "Visual field examination method using virtual reality glasses compared with the Humphrey perimeter," *Clin. Ophthalmol.*, vol. 11, pp. 1431–1443, Aug. 2017.
[14] M. Montelongo, A. Gonzalez, F. Morgenstern, S. P. Donahue, and S. L. Groth, "A virtual reality-based automated perimeter, device, and pilot study," *Transl. Vis. Sci. Technol.*, vol. 10, no. 3, p. 20, Mar. 2021.
[15] K. Vinod and P. A. Sidoti, "Glaucoma care during the coronavirus disease 2019 pandemic," *Current Opinion Ophthalmol.*, vol. 32, no. 2, pp. 78–82, 2021.
[16] A. Sipatchin, S. Wahl, and K. Rifai, "Eye-tracking for clinical ophthalmology with virtual reality (VR): A case study of the HTC vive pro eye's usability," *Healthcare*, vol. 9, no. 2, p. 180, Feb. 2021.
[17] T. Kimura, C. Matsumoto, and H. Nomoto, "Comparison of head-mounted perimeter and Humphrey field analyzer," *Clin. Ophthalmol.*, vol. 13, p. 501, Mar. 2019.
[18] R. Razeghinejad, A. Gonzalez-Garcia, J. S. Myers, and L. J. Katz, "Preliminary report on a novel virtual reality perimeter compared with standard automated perimetry," *J. Glaucoma*, vol. 30, no. 1, pp. 17–23, 2021.
[19] Z. S. Pradhan, T. Sircar, H. Agrawal, H. L. Rao, A. Bopardikar, S. Devi, and V. N. Tiwari, "Comparison of the performance of a novel, smartphone-based, head-mounted perimeter (GearVision) with the Humphrey field analyzer," *J. Glaucoma*, vol. 30, no. 4, pp. e146–e152, 2021.
[20] P. Kunumpol, N. Lerthirunvibul, P. Phienphanich, A. Munthuli, V. Tantisevi, A. Manassakorn, S. Chansangpetch, R. Itthipanichpong, K. Ratanawongphaibol, P. Rojanapongpun, and C. Tantibundhit, "GlauCUTU: Virtual reality visual field test," in *Proc. 43rd Annu. Int. Conf. IEEE Eng. Med. Biol. Soc. (EMBC)*, Nov. 2021, pp. 7416–7421.
[21] P. H. Artes, D. McLeod, and D. B. Henson, "Response time as a discriminator between true-and false-positive responses in suprathreshold perimetry," *Invest. Ophthalmol. Vis. Sci.*, vol. 43, no. 1, pp. 129–132, 2002.
[22] K. Guk, G. Han, J. Lim, K. Jeong, T. Kang, E. K. Lim, and *J. Jung*, "Evolution of wearable devices with real-time disease monitoring for personalized healthcare," *Nanomaterials*, vol. 9, no. 6, p. 813, 2019.
[23] *Material Safety Data Sheet: RA-25AB*, Infinite Crafts, Bangkok, Thailand, 2021.
[24] Zortrax. *Z-PLA Pro Safety Data Sheet*. Accessed: May 3, 2021. [Online]. Available: https://zortrax.com/filaments/z-pla-pro/
[25] P. R. K. Turnbull and J. R. Phillips, "Ocular effects of virtual reality headset wear in young adults," *Sci. Rep.*, vol. 7, no. 1, pp. 1–9, Dec. 2017.
[26] S. Peng, K. Liu, S.-G. Kuai, W. Zhou, X. Tang, Y. Shen, and X. Zhou, "Environmental influence on background luminance preference of computer use at home," in *Proc. ChinaSSL*, Nov. 2013, pp. 190–192.
[27] Extech and A FLIR Company. *LT300: Light Meter Extech Instruments*. Accessed: May 3, 2021. [Online]. Available: http://www.extech.com/products/LT300
[28] Calibration Laboratory. *Calibration Certificate Calibration Laboratory*. Accessed: May 3, 2021. [Online]. Available: https://www.calibrationlaboratory.com/en/standard
[29] Culture Hustle. *Black 3.0—The World's Blackest Black Acrylic Paint 150 ml*. Accessed: May 3, 2021. [Online]. Available: https://culturehustle.com/products/black-3-0-the-worlds-blackest-black-acrylic-paint-150ml
[30] H. K. Raut, V. A. Ganesh, A. S. Nair, and S. Ramakrishna, "Anti-reflective coatings: A critical, in-depth review," *Energy Environ. Sci.*, vol. 4, no. 10, pp. 3779–3804, 2011.

[31] C.-X. Qian, Q. Chen, Q. Cun, Y.-J. Tao, W.-Y. Yang, Y. Yang, Z.-Y. Hu, Y.-T. Zhu, and H. Zhong, "Comparison of the SITA faster—A new visual field strategy with SITA fast strategy," *Int. J. Ophthalmol.*, vol. 14, no. 8, pp. 1185–1191, Aug. 2021. [Online]. Available: https://pubmed.ncbi.nlm.nih.gov/34414082

[32] M. Kalloniatis and S. K. Khuu, "Equating spatial summation in visual field testing reveals greater loss in optic nerve disease," *Ophthalmic Physiol. Opt.*, vol. 36, no. 4, pp. 439–452, Jul. 2016.

[33] J. Phu, S. K. Khuu, B. V. Bui, and M. Kalloniatis, "A method using Goldmann stimulus sizes I to V—Measured sensitivities to predict lead time gained to visual field defect detection in early glaucoma," *Transl. Vis. Sci. Technol.*, vol. 7, no. 3, p. 17, Jun. 2018.

[34] H. L. Rao, V. U. Begum, D. Khadka, A. K. Mandal, S. Senthil, and C. S. Garudadri, "Comparing glaucoma progression on 24–2 and 10–2 visual field examinations," *PLoS ONE*, vol. 10, no. 5, May 2015, Art. no. e0127233.

[35] A. Heijl, V. M. Patella, L. X. Chong, A. Iwase, C. K. Leung, A. Tuulonen, G. C. Lee, T. Callan, and B. Bengtsson, "A new SITA perimetric threshold testing algorithm: Construction and a multicenter clinical study," *Amer. J. Ophthalmol.*, vol. 198, pp. 154–165, Feb. 2019.

[36] F. Eibe, M. A. Hall, and I. H. Witten, *The WEKA Workbench. Online Appendix for 'Data Mining': Practical Machine Learning Tools and Techniques*. San Mateo, CA, USA: Morgan Kaufmann, 2016.

[37] E. Frank, M. Hall, G. Holmes, R. Kirkby, B. Pfahringer, I. H. Witten, and L. Trigg, "Weka—A machine learning workbench for data mining," in *Data Mining and Knowledge Discovery Handbook*. Boston, MA, USA: Springer, 2009, pp. 1269–1277.

[38] K. He, X. Zhang, S. Ren, and J. Sun, "Deep residual learning for image recognition," in *Proc. IEEE Conf. Comput. Vis. Pattern Recognit. (CVPR)*, Jun. 2016, pp. 770–778.

[39] G. Holmes, A. Donkin, and I. H. Witten, "WEKA: A machine learning workbench," in *Proc. ANZIIS*, 1994, pp. 357–361.

[40] Y.-D. Zhang, X.-X. Hou, Y. Chen, H. Chen, M. Yang, J. Yang, and S.-H. Wang, "Voxelwise detection of cerebral microbleed in CADASIL patients by leaky rectified linear unit and early stopping," *Multimedia Tools Appl.*, vol. 77, no. 17, pp. 21825–21845, Sep. 2018.

[41] A. Ferreras, L. E. Pablo, D. F. Garway-Heath, P. Fogagnolo, and J. García-Feijoo, "Mapping standard automated perimetry to the peripapillary retinal nerve fiber layer in glaucoma," *Invest. Ophthalmol. Vis. Sci.*, vol. 49, no. 7, pp. 3018–3025, 2008.

[42] J. Yoo, H. Eom, and Y. S. Choi, "Image-to-image translation using a cross-domain auto-encoder and decoder," *Appl. Sci.*, vol. 9, no. 22, p. 4780, Nov. 2019.

[43] L. Li, Y. Fang, J. Wu, and J. Wang, "Autoencoder based residual deep networks for robust regression prediction and spatiotemporal estimation," 2018, *arXiv:1812.11262*.

[44] D. Mishkin and J. Matas, "All you need is a good init," 2015, *arXiv:1511.06422*.

[45] D. P. Kingma and J. Ba, "Adam: A method for stochastic optimization," 2014, *arXiv:1412.6980*.

[46] E. Hodapp, R. K. Parrish, and D. R. Anderson, *Clinical Decisions in Glaucoma*. Maryland Heights, MO, USA: Mosby, 1993.

[47] B. Bengtsson and A. Heijl, "A visual field index for calculation of glaucoma rate of progression," *Amer. J. Ophthalmol.*, vol. 145, no. 2, pp. 343–353, Feb. 2008.

[48] K. L. Gwet, "Computing inter-rater reliability and its variance in the presence of high agreement," *Brit. J. Math. Statist. Psychol.*, vol. 61, no. 1, pp. 29–48, 2008.

PATTHAPOL KUNUMPOL (Member, IEEE) received the B.E. degree in electrical engineering from Thammasat University, Bangkok, Thailand, in 2016. His research interests include virtual reality technology, pattern recognition, and machine learning.

NICHAPA LERTHIRUNVIBUL is currently pursuing the Medical degree with the Faculty of Medicine, Thammasat University, Pathum Thani, Thailand. She is also a Researcher with the Center of Excellence in Intelligent Informatics, Speech and Language Technology. Her research interests include the use of artificial intelligence in healthcare and medicine.

PHONGPHAN PHIENPHANICH (Member, IEEE) received the B.E. degree (Hons.) in computer engineering from the Suranaree University of Technology, Nakhon Ratchasima, Thailand, in 2009, and the M.E. degree in electrical engineering from Thammasat University, Bangkok, Thailand, in 2012, where he is currently pursuing the Ph.D. degree in computer engineering. He worked as a Co-Researcher with the National Electronics and Computer Technology Center (NECTEC), Thailand, from 2010 to 2012. His research interests include signal and speech processing, pattern recognition, and machine learning.

ADIREK MUNTHULI (Student Member, IEEE) received the B.E. degree in computer engineering and the M.E. degree in electrical and computer engineering from Thammasat University, Bangkok, Thailand, where he is currently pursuing the Ph.D. degree in computer engineering. His research interests include natural language processing, speech and signal processing, and machine learning.

KANJAPAT TEMAHIVONG received the M.D. degree (Hons.) from Chulalongkorn University, in 2019. He was awarded the Prince Mahidol Award Youth Program Scholarship to work as a Research Fellow at the Johns Hopkins University School of Medicine's Department of Ophthalmology-Low vision service, in 2021. He is currently a Medical Educator at the Chulalongkorn Healthcare Advanced Multi-Profession Simulation Center and a Researcher at the Glaucoma Research Unit, Department of Ophthalmology, Chulalongkorn University and the Center of Excellence in Intelligent Informatics, Speech and Language Technology, and Service Innovation. His research interests include virtual reality technology, perimetry and innovations in glaucoma diagnosis.

VISANEE TANTISEVI received the Medical degree (Hons.) from Chulalongkorn University, Bangkok, Thailand, and the Diploma degree in Ophthalmology and Glaucoma Fellowship training from King Chulalongkorn Memorial Hospital, Bangkok. Later, she received the Certificate in Clinical Glaucoma Fellowship from The Royal Victorian Eye and Ear Hospital, Centre for Eye Research Australia (CERA), University of Melbourne, Australia. She currently holds a number of appointments, including an Associate Professor of ophthalmology, the Deputy Chairperson of International Affairs, a Senior Instructor, a Residents' Advisory Board & Postgraduates Subcommittee, a Chief, and a Consultant of the Glaucoma Unit, Department of Ophthalmology, Faculty of Medicine, Chulalongkorn University. She is also a Glaucoma Consultant at the Queen Sirikit National Institute of Child Health and top-tier private hospital in Bangkok. She is the Head of Public Relations and International Affairs with the Thai Glaucoma Society (ThGS), a Sub-Committee of Academic Affairs of The Royal College of Ophthalmologists of Thailand (RCOPT), and a Regular Invited Reviewer for several peer-reviewed journals in ophthalmology. In addition, she is the Current Deputy Secretary General of the Asia Pacific

Glaucoma Society. She also carries a lot of experiences in many fields. She has been doing, mentoring and participating in glaucoma diagnosis and therapeutic researches both locally and internationally. Under her advisement, one of the advisees was granted Prince Mahidol Youth Award, the renowned prestigious fund for medical student project. She has been entrusted to lead the organizing team of numerous national and international scientific meetings in which acclaimed at high success as well as being invited to speak and chair sessions in various national and international scientific conferences.

ANITA MANASSAKORN received the Medical degree, in 1998. She completed Residency Training in ophthalmology from Chiang Mai University, in 2003. She finished a Clinical Research Fellowship in glaucoma from the University of California at Los Angeles, Los Angeles, CA, USA, and the University of Pittsburgh Medical Center, in 2004 and 2005. She is currently a Faculty Member at the Glaucoma Unit, Department of Ophthalmology, Faculty of Medicine, Chulalongkorn University, and King Chulalongkorn Memorial Hospital. Her research interests include glaucoma imaging, artificial intelligence in glaucoma imaging, diagnosis, and management.

SUNEE CHANSANGPETCH received the M.D. degree (Hons.) from Chulalongkorn University, Bangkok, Thailand, in 2007, the B.P.H. degree in public health administration from Sukhothai Thammathirad University, Bangkok, in 2010, and the Higher Grad. Dip. of Clin Sc. degree in ophthalmology from Chulalongkorn University, in 2012. She completed her Ophthalmology Residency and Glaucoma Fellowship at King Chulalongkorn Memorial Hospital, in 2012 and 2014, respectively. In 2018, she finished a Clinical Research Fellowship in glaucoma at the University of California at San Francisco, San Francisco, CA, USA. She is currently a Board-Certified Ophthalmologist at King Chulalongkorn Memorial Hospital and works as a Faculty Member at the Department of Ophthalmology, Chulalongkorn University. Her research interests include ocular biomechanics, glaucoma imaging, and innovations in glaucoma diagnosis.

RATH ITTHIPANICHPONG received the Doctor of Medicine degree at Siriraj Hospital, Mahidol University, in 2006. He has completed his Ophthalmology Residency Training and Glaucoma Fellowship Training at King Chulalongkorn Memorial Hospital, in 2014 and 2015, respectively. From his keen interest in low vision rehabilitation, he has completed the Clinical Fellowship Training in vision rehabilitation at the Wilmer Eye Institute, Johns Hopkins University School of Medicine, in 2018. He is currently an Instructor in ophthalmology at the Department of Ophthalmology, Chulalongkorn University, Bangkok, Thailand. His work has been related to both glaucoma and low vision field. From his passion in technology and innovation, he is also developing new technology to help improve quality of care in ophthalmology patients. He received the Prof. Tano Award for Young Ophthalmologist from the Asia Pacific Academy of Ophthalmology (APAO) in 2014. He also won the First Runner-Up Award for ICO World Ophthalmology Quiz 2014 at the World Ophthalmology Congress (WOC).

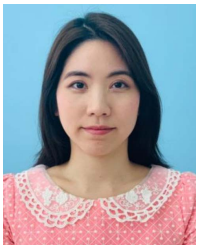

KITIYA RATANAWONGPHAIBUL received the M.D. (Hons.) and Higher Grad. Dip. of Clin Sc. degrees in ophthalmology from Chulalongkorn University, Bangkok, Thailand, in 2010 and 2016, respectively. She completed her Ophthalmology Residency and Glaucoma Fellowship at King Chulalongkorn Memorial Hospital, in 2016 and 2018, respectively. In 2019, she finished a Clinical Research Fellowship in glaucoma at the Harvard Medical School, Boston, MA, USA. She is currently a Board-Certified Ophthalmologist at King Chulalongkorn Memorial Hospital and works as a Faculty Member at the Department of Ophthalmology, Chulalongkorn University. Her research interests include innovations in glaucoma diagnosis and treatment, deep learning in ophthalmology, and medical education.

PRIN ROJANAPONGPUN received the bachelor's degree in science (B.Sc.) and the Medical degree (M.D.) from Chulalongkorn University. He did his Ophthalmology Residency at the Chulalongkorn University and the King Chulalongkorn Memorial Hospital. He pursued his Clinical Glaucoma Fellowship at the University of British Columbia under Prof. Stephen Drance. He also did Short Glaucoma Visiting Fellowship at the Bascom Palmer Eye Institute, Duke University, and New York Eye and Ear Infirmary. He is currently an Associate Professor of ophthalmology and an Immediate Past-Chairperson at the Department of Ophthalmology, Chulalongkorn University and King Chulalongkorn Memorial Hospital. He is also a Consultant at Bumrungrad International, Sukumvit Hospital, and MedPark Hospital, Bangkok, Thailand. He is an International Awardee from ASCRS, AAO, APAO, APACRS, and the Red Cross Society. He also received a Japanese Ophthalmological Society Scholarship to Dokkyo University, Japan. He is the Current President of the Asia Pacific Glaucoma Society (APGS), a Board of Trustee of the International Council of Ophthalmology (ICO), a Regional Advisory Committee of American Academy of Ophthalmology (AAO), the Council of the Asia Pacific Academy of Ophthalmology (APAO), a Steering Committee of the World Glaucoma Association (WGA), an Executive Board of the Royal College of Ophthalmologists of Thailand, an Immediate Past President of Thai Glaucoma Society, and a Past President of the South East Asia Glaucoma Interest Group (SEAGIG) and Asian Angle Closure Glaucoma Club (AACGC). He also serves as a chair, a committee, and a consultant to many national and regional societies and industries. He is a Key Opinion Leader in glaucoma, combined cataract and glaucoma surgery, advanced cataract surgery, and IOL customization.

CHARTURONG TANTIBUNDHIT (Member, IEEE) received the B.E. degree in electrical engineering from Kasetsart University, Bangkok, Thailand, in 1996, and the M.S. degree in information science and the Ph.D. degree in electrical engineering from the University of Pittsburgh, Pittsburgh, PA, USA, in 2001 and 2006, respectively. Since 2006, he has been working with Thammasat University, Thailand, where he is currently an Associate Professor with the Department of Electrical and Computer Engineering, and the Head of the Speech and Language Technology Cluster, Center of Excellence in Intelligent Informatics, Speech and Language Technology, and Service Innovation (CILS). From 2007 to 2008, he was a Postdoctoral Researcher with the Signal Processing and Speech Communication Laboratory (SPSC), Graz University of Technology, Graz, Austria. His research interests include handcrafted machine learning and deep learning in medicine, biomedical signal processing, and speech processing. He was the IEEE ICASSP Student Paper Contest Winner in 2006. He led a team that won the Grand Prix from the 45th International Exhibition of Inventions of Geneva in 2017.